Urban determinants of COVID-19 spread: A comparative study across three cities in New York State

**Noname manuscript No.**
(will be inserted by the editor)

# Urban determinants of COVID-19 spread: A comparative study across three cities in New York State

**A. Truszkowska · M. Fayed · S. Wei · L. Zino · S. Butail · E. Caroppo · Z.-P. Jiang · A. Rizzo · M. Porfiri**

Received: date / Accepted: date

**Abstract** The ongoing pandemic is laying bare dramatic differences in the spread of COVID-19 across seemingly similar urban environments. Identifying the urban determinants that underlie these differences is an open research question, which can contribute to more epidemiologically resilient cities, optimized testing and detection strategies, and effective immunization efforts. Here, we perform a computational analysis of COVID-19 spread in three cities of similar size in New York State (Colonie, New Rochelle, and Utica) aiming to isolate urban determinants of infections and deaths. We develop detailed digital representations of the cities and simulate COVID-19 spread using a complex agent-based model, taking into account differences in spatial layout, mobility, demographics, and occupational structure of the population. By critically comparing pandemic outcomes across the three cities under equivalent initial conditions, we provide compelling evidence in favor of the critical role of hospitals. Specifically, with highly efficacious testing and detection, the number and capacity of hospitals, as well as the extent of vaccination of hospital employees are key determinants of COVID-19 spread. The modulating role of these determinants is reduced at lower efficacy of testing and detection, so that the pandemic outcome becomes equivalent across the three cities.

**Keywords** Agent-based model · COVID-19 · Resilient cities · Urban design

A. Truszkowska
Center for Urban Science and Progress, Tandon School of Engineering, New York University, Brooklyn NY, USA
Department of Mechanical and Aerospace Engineering, Tandon School of Engineering, New York University, Brooklyn NY, USA

M. Fayed
New York University Abu Dhabi, United Arab Emirates

S. Wei
Center for Urban Science and Progress, Tandon School of Engineering, New York University, Brooklyn NY, USA

L. Zino
Faculty of Science and Engineering, University of Groningen, Groningen, The Netherlands

S. Butail
Department of Mechanical Engineering, Northern Illinois University, DeKalb IL, USA

E. Caroppo
Department of Mental Health, Local Health Unit ROMA 2, Rome, Italy
University Research Center He.R.A., Università Cattolica del Sacro Cuore, Rome, Italy

Z.-P. Jiang
Department of Electrical and Computer Engineering, Tandon School of Engineering, New York University, Brooklyn NY, USA

A. Rizzo
Department of Electronics and Telecommunications, Politecnico di Torino, Turin, Italy
Institute for Invention, Innovation and Entrepreneurship, Tandon School of Engineering, New York University, Brooklyn NY, USA

M. Porfiri
Center for Urban Science and Progress, Tandon School of Engineering, New York University, Brooklyn NY, USA
Department of Mechanical and Aerospace Engineering, Tandon School of Engineering, New York University, Brooklyn NY, USA
Department of Biomedical Engineering, Tandon School of Engineering, New York University, Brooklyn NY, USA
E-mail: mporfiri@nyu.edu

## 1 Introduction

World-wide urban areas remain the major targets of the ongoing COVID-19 pandemic due to their high population densities, frequent human interactions, and daily commutes [1,2]. Analyzing the spread in metropolitan areas can help alleviate the epidemiological burden, by supporting the design of policies for detection [3–5], immunization [6,7], and intervention [8,9]. Alongside with scientifically backed policy-making, research on COVID-19 spread in urban environments can support the identification of factors that reduce vulnerability to future pandemics [10] and create epidemiologically-resilient cities [11,12]. Predictably, population density has been proposed as an important determinant of the spread [13–15]. Empirical studies have also demonstrated the impact of demographics [16–19], socio-economic factors [20,21], and climate [22] on the local spread of the pandemic.

While evidence-based analysis is key to assess the current state of the pandemic and identify causal associations, computational models of COVID-19 spread have been instrumental in the simulation of several what-if scenarios that have shaped public health policies across the globe [23–27]. With a strong focus on major urban areas, these models have helped quantify the benefits of non-pharmaceutical interventions [28–30], identify optimal schemes for prioritizing and administering vaccines [31–35], understand the implications of human mobility [36–38], and devise safe reopening strategies for the economy [39–42].

Several studies have investigated the spread in urban environments, in search of characteristics that influence the spread, often towards informing data-driven models. For example, Bhowmik *et al.* [43] performed a county-level analysis of the United States and proposed a model of COVID-19 spread that is informed by demographics, socio-economic factors, and healthcare availability. Aguilar *et al.* [44] analyzed different types of urban layouts with respect to spread dynamics and effectiveness of mobility restrictions. Through simulations of an infectious disease in synthetic cities with different geographical layouts, Brizuela *et al.* [45] demonstrated that heterogeneous urban design may lead to a highly non-uniform distribution of the epidemic, potentially targeting the most vulnerable. In a study of 163 cities across the World, Hazarie *et al.* [46] discovered that COVID-19 contagion increases proportionally to human mobility in densely populated areas. Li et al. [47] proposed a series of major urban fabric contributors to the initial COVID-19 epidemic in Wuhan, including the distribution of public facilities, hospitals, roads, and subway stations.

In this work, we complement these efforts through a high-resolution computational model at the granularity of a single individual for the spread of COVID-19 in three different cities in New York State: Colonie, New Rochelle, and Utica. These cities are selected for their similar size, but also because they differ by geographic layouts, population density of their residents, demographics, socio-economic characteristics, and mobility patterns within their populations [48]. COVID-19 spread is simulated within each city using an agent-based model, which builds upon our previous work [34, 35,42]. By modeling the cities under equivalent initial conditions for the contagion, we can successfully distill urban determinants of COVID-19 spread. Unique to this study is the estimation of the extent to which different location types influence infections and deaths, by selectively excluding one of them at a time from the analysis. Likewise, we also detail the specific role of different agents in the spread in hospitals, from COVID-19 patients to staff.

Our results confirm the key role of testing and detection on the ability to shape the spread across different urban environments. As highly efficacious testing and detection is attained, our model projections suggest a crucial effect of the number and capacity of hospitals on the spread of the virus, making cities with large and concentrated sanitary hubs more effective to combat the spread than those with more scattered and smaller hospitals. Moreover, vaccination of hospital employees seems to be a further salient factor that contributes to halting the spread. The modulating role of these factors is reduced for lower testing and detection efficacy, whereby poor detection and testing lead to substantially equivalent COVID-19 spreading dynamics across the three cities. Our work highlights the importance of testing and the need for reducing the spread from the hospitals through case isolation and immunization of the personnel. Urban planning should consider the location and structure of hospitals, which may be critical in containing the pandemic.

## 2 Methods

Our computational framework consists of two components: a detailed database of the cities and their population, and an agent-based model of COVID-19 spread with the resolution of the single individual. The core framework is described in our earlier publications [34,35, 42], to which we point the interested reader for further details.

### 2.1 Database

The database of each city contains the coordinates of all the public and residential buildings along with resident demographics. With this information, we are able to recreate synthetic cities – the fabric upon which software agents mimicking individuals will live, interact, and contract the infection. The locations of schools, retirement homes, and hospitals were collected using OpenStreetMap [49] and Google Maps [50]. The number of students in each primary, middle, and high school was estimated using the data from the National Center of Education Statistics [51]. Capacities of daycares were assessed using the U.S. child care database and building sizes [52–54]. The number of students in colleges and the number of residents of retirement homes were estimated using websites of specific institutions. The number of in-patients in hospitals due to conditions other than COVID-19 in New Rochelle and Utica represented about 60% of the bed capacity recorded by New York State Department of Health [55] and the American Hospital Directory [56]. For Colonie, we hypothesized that hospitals would be able to treat COVID-19 patients, although, in practice, these hospitals were clinics that do hospitalize patients. Consistent with the premise of lack of hospitalization, we assumed that none of the virtual bed capacity of Colonie was allocated to non-COVID-19 patients.

The residents work in and outside of their city; their workplace locations were determined using the U.S. Census data [48] and SafeGraph [57]. The public transit commute patterns were gathered from Google Maps [50]. Our model also includes various non-essential businesses and locations, such as restaurants, malls, and grocery stores. Similar to workplaces, non-essential business locations were determined using SafeGraph [57]. The database also includes several major schools, retirement homes, or hospitals located in close proximity of the city but outside its administrative boundaries due to the high likelihood of residents using and frequenting those places. All the private and public modeled locations are displayed in Figure 1a).

The geographic coordinates of residential buildings were collected using ArcGIS [58], without distinguishing the number of individual units in each residential building. A proxy for the distribution of buildings with multiple units was instantiated in our model using the U.S. Census data [48]. While the local layout of such units may differ from the real one, we made sure that the real and the modeled distributions are statistically equivalent. This procedure simplifies our previous approach [34, 42], in which all the building locations and types were manually collected, toward the systematic automation of the data collection phase. Details of this approach for the collection of site locations and the verification of its validity with respect to the manual collection technique proposed in [34, 42] are described in the Supplementary Material.

To recreate city populations we used the U.S. Census data on age distribution, household and family structure, commute times and modes, and employment characteristics [48]. All the generic workplaces and agents working in them were divided into five occupational categories, as shown in Figure 1b). Such a fine categorization is an important improvement with respect to our previous work [34, 42], in which we only distinguished between schools, retirement homes, and hospital employees [34, 42].

The rationale for such a fine categorization lies in the need to capture the different employment structure of the three cities and the corresponding variation of workplace-related infection risks. In our model, we explicitly simulate COVID-19 spread in the workplaces that are in the cities. Each of these locations has an assigned occupational category and a category-specific transmission rate, contributing to the infection risk for all the agents employed therein. Contrarily, the occupational category of an agent who works outside of city is a characteristic of the agent, rather than the location. This stems from the fact that our model avoids simulations of the entire region by approximating the contagion in the out-of-city locations. The workplace-related infection risk for an agent working out-of-city corresponds to the estimated fraction of infected people in the region multiplied by occupation type transmission rate. Overall, the employment type distribution matches the U.S. Census [48] data with details on its distribution and rate computation enclosed in the Supplementary Material.

The age distributions of the cities' residents are shown in Figure 1c), while other characteristics of the cities are summarized in Table 1. The three cities differ in some characteristics, such as spatial layout, population density, fraction of residents in the 0–9 age cohort, unemployment rates, commute patterns, workplace locations, and percentage of people working in low- versus high-risk occupations. At the same time, the three cities have similar household and family structure and age distribution of older children and adults.

### 2.2 Agent-based model

In our model, each city resident is represented by a simulated agent who mirrors residents' lifestyles. The agents could live together in distinct households, retirement homes, and be admitted to hospitals. They could work,

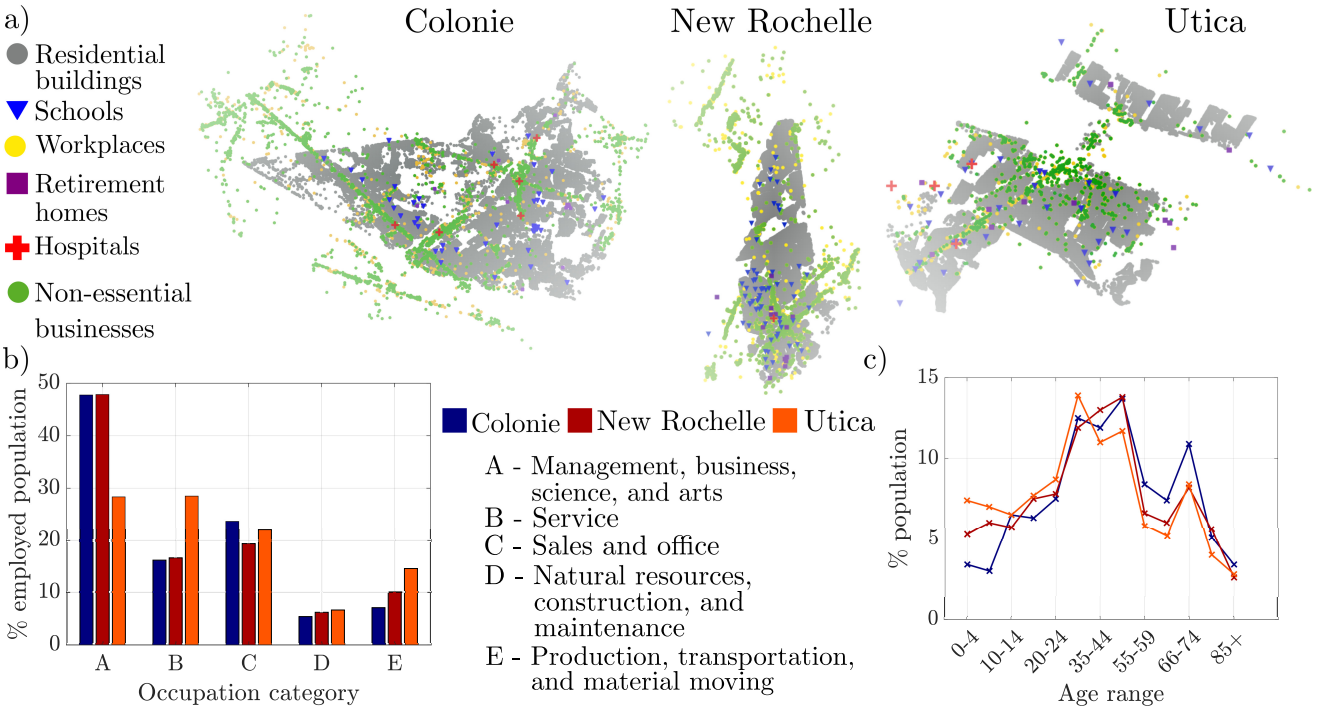


**Fig. 1** a) Public and residential locations in the three cities that are considered in the model, b) occupation categories of the employed residents, and c) age distribution of the population.

**Table 1** Characteristics of the three modeled cities.

| | Colonie | New Rochelle | Utica |
|---|---|---|---|
| Population | 82,797 | 79,205 | 59,750 |
| Population/sqmi | 1,459 | 7,445 | 3,714 |
| Unemployment rate | 3.1% | 6.1% | 8.2% |
| Use of public transit | 1.02% | 8.5% | 0.77% |
| Workers out of the city | 19.7% | 31.2% | 15.6% |

go to school, visit non-essential businesses, visit each other, and travel to work through various transit means, consistent with the database described in Section 2.1.

COVID-19 spreads through contacts that agents make in the locations they visit through a probabilistic mechanism. Specifically, the transmissibility of COVID-19 is dependent on the location type and agent role and is quantified through transmission rates, as explicitly detailed in our previous work [34,42]. To capture the transmission levels associated with different occupations, we use the empirical data published by the Washington State Department of Health [59,60]. Details about this procedure and exact values of the infected fractions and rates are included in the Supplementary Material.

Once infected, agents can develop symptoms or remain asymptomatic. Infected agents (both asymptomatic and symptomatic) and those with symptoms similar to COVID-19 but from other diseases can be tested with a certain probability. We refer to this likelihood as testing and detection efficacy (low, moderate, or perfect). A low efficacy corresponds to the detection of 63% of the symptomatic agents and 44% of the asymptomatic, following our model calibration for the first wave [34]. Moderate efficacy implies that 82% of symptomatic and 72% of asymptomatic agents are detected, and perfect efficacy means that all infected agents are tested. With the exception of hospital employees, when an agent "signs up" for a test, they are immediately home-isolated. This mimics local practices, whereby healthcare staff do not isolate until they are confirmed COVID-19 positive or develop symptoms of the disease. Tests are performed in hospitals or in independent testing sites, where the latter locations are assumed to pose no risk of transmission. Agents who tested positive can be treated at home, through routine hospitalization, or in ICUs, depending on the severity of the disease, which is determined in a stochastic fashion, consistent with COVID-19 clinical data [61]. The disease progression terminates with either a recovery or death. The exact COVID-19 progression used in this work follows the progression model described in [42].

Similar to our previous work [42], our model contemplates vaccination for agents. In our simulations, we mimic a continuously progressing vaccination campaign. A portion of the agents is immunized at the beginning of the study and the number of vaccinated individuals increases linearly as the simulation progresses. Once

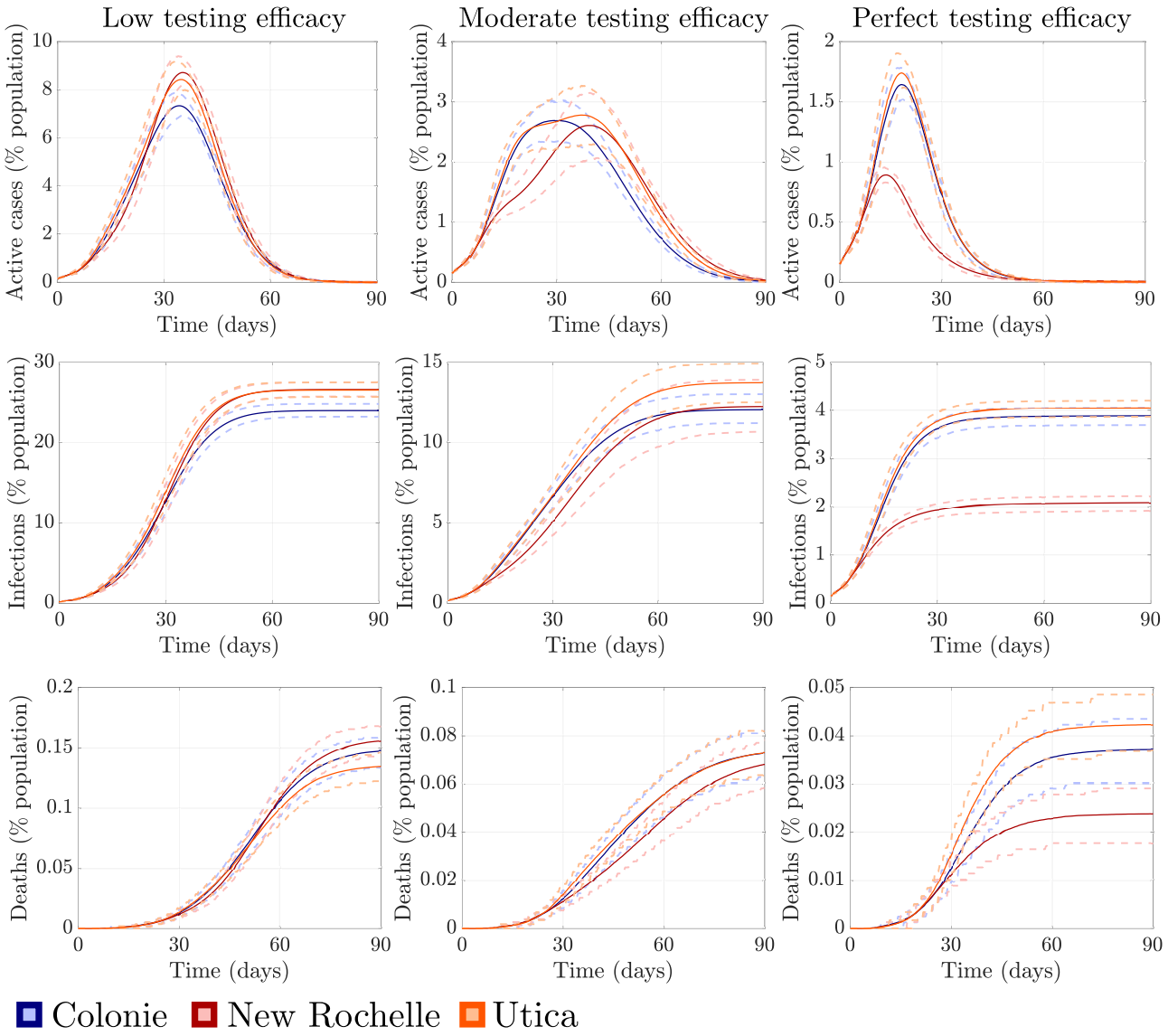


**Fig. 2** Simulations of the spread of COVID-19 in Colonie (blue curves), New Rochelle (red curves), and Utica (orange curves) over a time-window of three months, for three different testing and detection efficacies. Solid lines represent the average of of 400 independent realizations; dashed lines are the $25^{\text{th}}$ and $75^{\text{th}}$ percentiles.

vaccinated, we assume that individuals are granted full immunity to COVID-19. Despite being simplistic, such an assumption should be realistic for the short-term simulation window (through Summer 2021) considered in this work. Non-ideal effectiveness of vaccines and waning immunity has been incorporated within our simulation framework in a separate publication [35].

The core parameters used in the model are described in detail in our previous works. Following our most recent study [35], we simulate the Delta variant of the virus with epidemiological parameters calibrated on clinical estimations [62,63]. Because our goal was to analyze the impact of non-epidemiological factors, such as population density and employment distributions, on the spread of COVID-19, all three cities were simulated with the same initial percentage of infected agents, patients in various stages of COVID-19, and vaccinated agents, chosen uniformly at random in the population. All cities are assumed to have the same risk levels from travels from and to neighboring cities, transmission in public transit, and frequency of visiting non-essential business locations. The detailed parameter list is enclosed in the Supplementary Material.

## 3 Results

### 3.1 COVID-19 spread in the three cities

Starting from the same initial conditions, we simulated three months of COVID-19 spread in the three cities for different testing and detection efficacies. Since the initialization of the system and the contagion model are governed by probabilistic mechanisms, for each analyzed condition, we estimated the outcome of the spreading process via Monte Carlo simulations, by averaging over 400 independent realizations. Results shown in Figure 2 indicate that under low and moderate testing and detection efficacy, the three cities of Colonie, New Rochelle, and Utica do not experience significant differences in the COVID-19 toll, either in terms of total infections or in total deaths. However, under perfect efficacy, the case and death counts in New Rochelle are considerably smaller than in the other two cities.

### 3.2 Identification of major COVID-19 hubs under perfect testing and detection efficacy

To shed light on the factors that determine the significantly lower spread in New Rochelle for perfect testing and detection efficacy, we performed two additional analyses. In the first analysis, we selectively excluded different location types from the spread by assuming that no transmission can happen in that type of locations (formally, by setting the corresponding transmission rate to 0). In this way, we simulated the spread in the three cities without agents being infected at generic workplaces, schools, hospitals, retirement homes, or non-essential business locations, respectively.

According to the results shown in Figure 3, the spread in Colonie and Utica are comparable to the one in New Rochelle only if hospitals are excluded from transmission. This result can be traced back to different rules applied to hospital employees compared to the general population. Under perfect testing and detection efficacy, nearly all the agents who become infected during the simulated time-window are successfully detected. However, as opposed to any other agent, hospital employees do not home-isolate before receiving their positive test result or developing disease symptoms. As such, they are allowed a wider period for potentially spreading the infection in the hospital and outside. Furthermore, New Rochelle has only one hospital with 345 employees, which is much less than Colonie (six hospitals, 1,552 employees) and Utica (four hospitals, 962 employees). As such, New Rochelle provides less routes for COVID-19 to spread from hospital employees who are positive but still performing their duties.

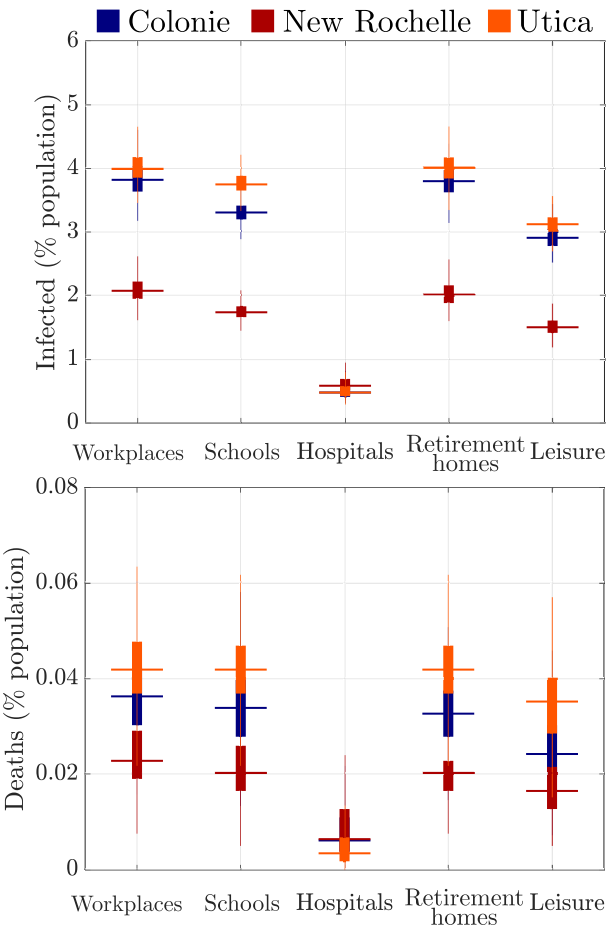


**Fig. 3** Final COVID-19 toll (infections and deaths) after simulating a three-month window and excluding the indicated location types from the spread. The bottom and top edges of the box plots mark the $25^{\text{th}}$ and $75^{\text{th}}$ percentiles, the solid lines represent the median, and the whiskers span the entire, outlier-free dataset.

While our simulation results are suggestive of a key role of hospital in relaying the infection *outside* of their facilities, the question about possible causes of transmission *within* facilities, with the associated risk of generating outbreaks, remains open. To this aim, our second analysis sought to identify the types of agents that contributed the most to the spread within hospitals. In particular, we performed a series of simulations where we excluded from the transmission dynamics select types of agents in hospitals. The types of agents that we excluded were patients who were originally admitted to the hospital due to conditions other than COVID-19, agents that get tested at a hospital, hospital employees, routinely hospitalized COVID-19 patients, and patients treated for COVID-19 in an ICU, respectively. The results in Figure 4 show that the reduction of spread in Colonie and Utica is achieved only when excluding the agents who are routinely hospitalized for COVID-19,

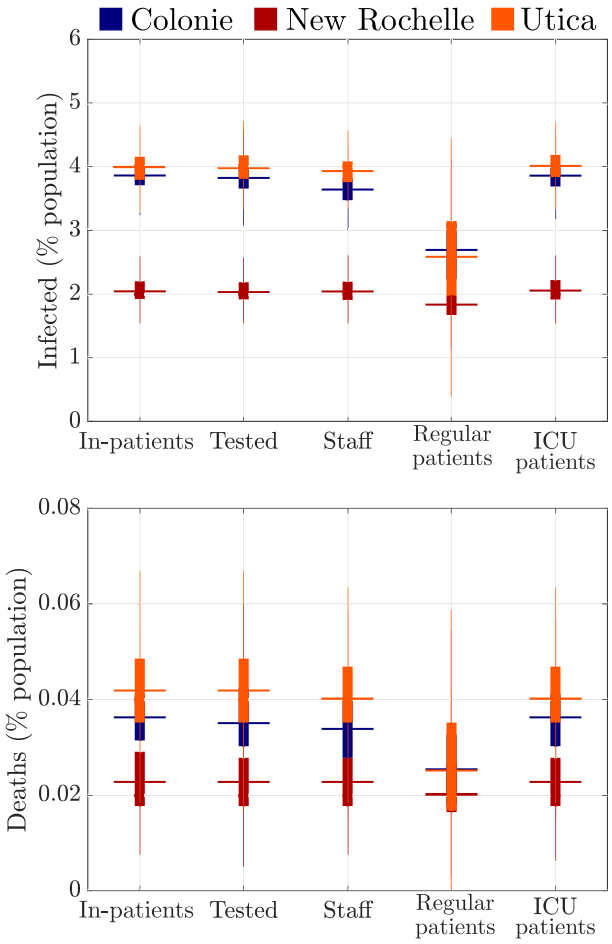


**Fig. 4** Final COVID-19 toll (infections and deaths) after simulating a three-month window and excluding the indicated agent type from the spread within hospitals. *In-patients* refer to agents originally admitted to the hospital due to conditions other than COVID-19, *Tested* are agents having their test in a hospital, *Staff* are the healthcare employees, *Regular patients* are the agents routinely hospitalized for COVID-19, and *ICU patients* are the agents treated for COVID-19 in ICUs. The bottom and top edges of the box plots mark the 25th and 75th percentiles, the solid lines represent the median, and the whiskers span the entire, outlier-free dataset.

suggesting their prominent role as main spreaders within hospital facilities.

### 3.3 Effect of vaccinating hospital employees

Results in Figure 4 leads us to formulate the hypothesis that an important route for COVID-19 generates from hospitals, among patients, and spreads outside, due to infected employees who could interact with others between the time the infection is contracted and the emergence of symptoms or the positive outcome of a test. Under this premise, it becomes of paramount importance to vaccinate hospital employees.

To further back this claim, we performed an additional simulation in which we vaccinated all the initially healthy hospital employees. Under the assumption of perfect immunity, results in Figure 5 confirm that vaccination of healthcare employees greatly reduces the toll of the epidemic. Importantly, the immunity of hospital employees also changes the previous trends, with Colonie presenting the least number of cases due to its larger number of hospital and hospital employees. Given that the vaccines in reality do not fully protect against COVID-19 and their effects wane with time, this best-case scenario further highlights the need of mandatory (or extremely incentivized) immunization of healthcare workers.

## 4 Discussion

Our work offers a unique, comparative study of different U.S. cities toward elucidating the urban determinants of COVID-19 spread. Through a high-resolution agent-based model, we simulated the spread of COVID-19 in three similar-sized cities in New York state (Colonie, New Rochelle, and Utica), differing in spatial layout, population demographics and lifestyles, and occupational characteristics. We matched the initial COVID-19-related conditions in the three cities to facilitate the isolation of non-epidemiological, urban determinants. Acknowledging the critical importance of testing and detection in fighting the pandemic, our analysis included different testing and detection scenarios, from low (reminiscent of the first wave) to perfect efficacy.

Our computational results indicate that the three cities experience similar COVID-19 infections and deaths for low and moderate efficacies of testing and detection. In the case of perfect detection and testing efficacy, the COVID-19 toll in New Rochelle remarkably drops below the other two cities. Through additional analysis on the influence of different locations on the spread, we demonstrated that the reason behind this difference is due to the spread in hospitals. Specifically, we found that contagion within hospitals is dominated by routinely hospitalized COVID-19 patients and hospital employees who could serve as vectors from the hospitals out to the city. Predictably, our numerical simulations also indicate that vaccination of healthcare workers is successful in preventing these contagions, thereby reducing the COVID-19 toll in the three cities. Our results contribute a valuable outlook on testing, immunization, and isolation of infected cases in urban environments.

Overall, the results of our study highlight the importance of timely and efficacious testing and detection, consistent with claims from our previous analyses [34,

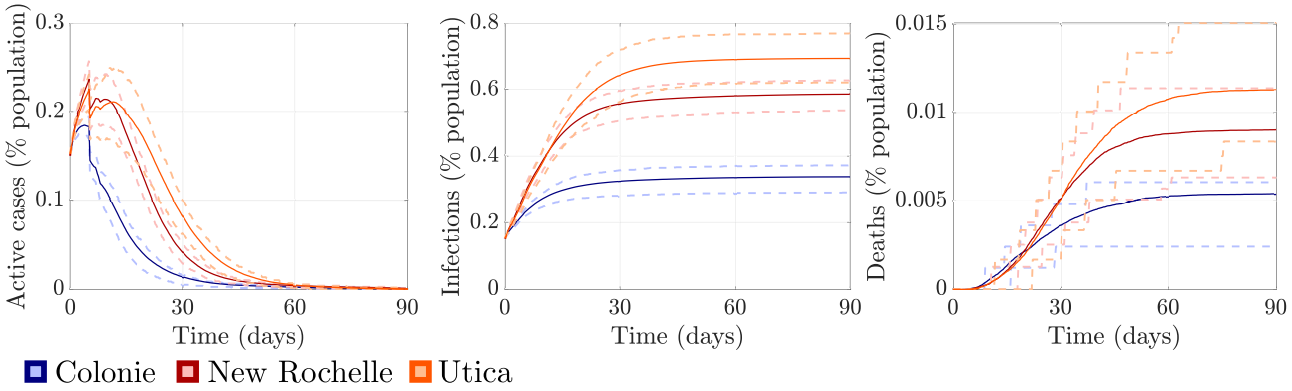


**Fig. 5** Spread of COVID-19 with perfect testing and detection and fully vaccinated hospital employees. Solid lines represent the mean out of 400 independent realizations. Dashed lines are the realizations corresponding to the $25^{\text{th}}$ and $75^{\text{th}}$ percentiles.

35,42] and work of other research groups [28,64]. By improving the efficacy of testing and detection from low to perfect, the case count drops as much as six fold, resulting in up to five times fewer deaths. With reduced testing and detection, differences between the fabrics of the cities have a limited impact on COVID-19, resulting in equivalent epidemic patterns. In this vein, despite their differences, the burden of undetected cases bears similar, dramatic consequences on the three cities. These claims are aligned with strategic plans implemented world-wide in an effort to curb the COVID-19 pandemic through immunization and non-pharmaceutical interventions [65, 66].

With perfect testing and detection efficacy, New Rochelle had, on average, two times less infection cases and deaths compared to Colonie and Utica. We attribute this variation to differences in COVID-19 spread in hospitals. The severity of the spread in hospitals has been documented by other works [67–70], while hospitals have been identified as dominant COVID-19 hubs have been identified in various computational studies [47,71]. With respect to urban planning and epidemiological crisis mitigation, our results highlight the importance of proper isolation of the hospitalized infected individuals [69, 72]. Following successful implementations [73–75], cities should consider establishing fewer, more isolated hospitals to treat COVID-19 patients. Ongoing solutions aiming to reduce COVID-19 spread from hospitals is the utilization of mobile pre-screening applications before a visit [76], and delegating some of the diagnostic services to online meetings rather than live interactions [77].

In our model, only hospital employees spread COVID-19 from the hospitals to the general population, which is consistent with restrictions that are placed in health care facilities on guests' admission and efforts to perform remote diagnosis when possible [77,78]. The intensity of the spread is linked to the nature of their work, preventing hospital employees from quarantining unless tested positive or developing symptoms [79,80]. Vaccinating these individuals in our simulations resulted in twenty times fewer cases and ten times less casualties. While we have assumed that vaccines grant full, long-lasting immunity, it is tenable that equivalent, albeit reduced, benefits would persist under more realistic conditions, in line with other studies [67,68]. The importance of vaccinating healthcare workers pointed out in our study is particularly relevant, as many governments across the globe are hesitant in mandating their immunization [81, 82], facing criticism from the employees and the public.

When interpreting the results of our work, one should keep in mind several of its limitations. First, our testing and detection procedure is very conservative, with agents isolating as soon as they decide to get tested. This is likely a more optimistic scenario than what is encountered in reality, especially after relaxing local quarantine rules for the fully vaccinated [83]. Second, the model does not accommodate any form of contact tracing, which is still a major component of COVID-19 curbing. Third, the vaccines are also assumed to act in an idealized fashion, and there are no limits to their application, like agents' age or hesitancy. Fourth, our model does not account for additional deaths that may result from the overburden of hospitals and the reduction of hospital employees due to infection. Adding such a feature may partly reduce differences in the number of deaths between the three cities.

In conclusion, our study indicates that enhancing the effectiveness of testing and detection policies would make urban determinants essential factors of the epidemic outcome. Conversely, prioritizing urban modifications over improvement on testing may nullify such an effort. In the absence of highly efficacious testing and detection, cities appear to be equivalently vulnerable to COVID-19 spread. If highly efficacious testing and detection are practiced, our analysis points to hospitals as major sources of epidemic spread, with hospitalized

individuals causing local outbreaks and employees facilitating the spread across the community. Our results imply that an epidemiologically resilient city should possess well-developed detection infrastructure providing high-quality and timely tests; fewer, dedicated healthcare facilities that provide good isolation of treated individuals; and strongly incentivized vaccination of its healthcare workers.

**Acknowledgements** The work of AT, EC, ZPJ, AR, and MP was partially supported by the National Science Foundation (CMMI-2027990). The work of SB was partially supported by National Science Foundation (CMMI-2027988). The funders had no role in study design, data collection and analysis, decision to publish, or preparation of the manuscript.

**Author contributions** Conceptualization: AT, LZ, SB, AR, MP; data curation: AT, MF, SW; methodology: AT, MF, SW, LZ, SB, AR, MP; software: AT, MF, SW; validation: AT, MF, SW; formal analysis: AT, LZ, SB, AR, MP; investigation: all the authors; resources: MP; writing—original draft preparation: AT, LZ, SB, AR, MP; writing—review and editing: EC, ZPJ; visualization: AT, MF, SW; supervision: SB, AR, MP; project administration: MP; funding acquisition: SB, ZPJ, AR, MP.

**Data availability statement** The database is accessible at `https://github.com/Dynamical-Systems-Laboratory/Multitown-Population-ABM` and the software used for the simulations is available at `https://github.com/Dynamical-Systems-Laboratory/DSL_ABM-Multitown`

## References

1. Ritchie Hannah, Mathieu Edouard, Rodés-Guirao Lucas, et al. Coronavirus Pandemic (COVID-19) *Our World in Data.* 2020. https://ourworldindata.org/coronavirus.
2. Nicolelis Miguel AL, Raimundo Rafael LG, Peixoto Pedro S, Andreazzi Cecilia S. The impact of super-spreader cities, highways, and intensive care availability in the early stages of the COVID-19 epidemic in Brazil *Scientific Reports.* 2021;11:1–12.
3. Borjas George J. Demographic determinants of testing incidence and COVID-19 infections in New York City neighborhoods *National Bureau of Economic Research preprint, 26952.* 2020.
4. Lieberman-Cribbin Wil, Tuminello Stephanie, Flores Raja M, Taioli Emanuela. Disparities in COVID-19 testing and positivity in New York City *American Journal of Preventive Medicine.* 2020;59:326–332.
5. Ransome Yusuf, Ojikutu Bisola O, Buchanan Morgan, Johnston Demerise, Kawachi Ichiro. Neighborhood Social Cohesion and Inequalities in COVID-19 Diagnosis Rates by Area-Level Black/African American Racial Composition *Journal of Urban Health.* 2021;98:222–232.
6. Lei Yuxiao. Hyper focusing local geospatial data to improve COVID-19 vaccine equity and distribution *Journal of Urban Health.* 2021;98:453–458.
7. Moreland Ashley, Gillezeau Christina, Alpert Naomi, Taioli Emanuela. Assessing influenza vaccination success to inform COVID-19 vaccination campaign *Journal of Medical Virology.* 2021.
8. Nomura Shuhei, Tanoue Yuta, Yoneoka Daisuke, et al. Mobility Patterns in Different Age Groups in Japan during the COVID-19 Pandemic: a Small Area Time Series Analysis through March 2021 *Journal of Urban Health.* 2021;98:635–641.
9. Bian Zilin, Zuo Fan, Gao Jingqin, et al. Time lag effects of COVID-19 policies on transportation systems: A comparative study of New York City and Seattle *Transportation Research Part A: Policy and Practice.* 2021;145:269–283.
10. Salama Ashraf M. Coronavirus questions that will not go away: interrogating urban and socio-spatial implications of COVID-19 measures *Emerald Open Research.* 2020;2.
11. Afrin S, Chowdhury FJ, Rahman MM. COVID-19 Pandemic: Rethinking Strategies for Resilient Urban Design, Perceptions, and Planning *Frontiers in Sustainable Cities.* 2021;3:668263.
12. Ellis Geraint, Grant Marcus, Brown Caroline, et al. The urban syndemic of COVID-19: insights, reflections and implications: Cities, health and COVID-19: editorial for the special issue *Cities & Health.* 2021:1–11.
13. Kadi Nadjat, Khelfaoui Mounia. Population density, a factor in the spread of COVID-19 in Algeria: statistic study *Bulletin of the National Research Centre.* 2020;44:1–7.
14. Wong David WS, Li Yun. Spreading of COVID-19: Density matters *Plos one.* 2020;15:e0242398.
15. Khavarian-Garmsir Amir Reza, Sharifi Ayyoob, Moradpour Nabi. Are high-density districts more vulnerable to the COVID-19 pandemic? *Sustainable Cities and Society.* 2021;70:102911.
16. Dowd Jennifer Beam, Andriano Liliana, Brazel David M, et al. Demographic science aids in understanding the spread and fatality rates of COVID-19 *Proceedings of the National Academy of Sciences.* 2020;117:9696–9698.
17. Khan Wasiq, Hussain Abir, Khan Sohail Ahmed, Al-Jumailey Mohammed, Nawaz Raheel, Liatsis Panos. Analysing the impact of global demographic characteristics over the COVID-19 spread using class rule mining and pattern matching *Royal Society Open Science.* 2021;8:201823.
18. Davies Nicholas G, Klepac Petra, Liu Yang, Prem Kiesha, Jit Mark, Eggo Rosalind M. Age-dependent effects in the transmission and control of COVID-19 epidemics *Nature Medicine.* 2020;26:1205–1211.
19. Ruprecht Megan M, Wang Xinzi, Johnson Amy K, et al. Evidence of social and structural COVID-19 disparities by sexual orientation, gender identity, and race/ethnicity in an urban environment *Journal of Urban Health.* 2021;98:27–40.
20. Buja Alessandra, Paganini Matteo, Cocchio Silvia, Scioni Manuela, Rebba Vincenzo, Baldo Vincenzo. Demographic and socio-economic factors, and healthcare resource indicators associated with the rapid spread of COVID-19 in Northern Italy: An ecological study *PLOS ONE.* 2020;15:e0244535.
21. Kranjac Ashley Wendell, Kranjac Dinko. County-level factors that influenced the trajectory of COVID-19 incidence in the New York City area *Health Security.* 2021.
22. Metelmann Soeren, Pattni Karan, Brierley Liam, et al. Impact of climatic, demographic and disease control factors on the transmission dynamics of COVID-19 in large cities worldwide *One Health.* 2021;12:100221.
23. Estrada Ernesto. COVID-19 and SARS-CoV-2. Modeling the present, looking at the future *Physics Reports.* 2020;869:1-51.
24. Vespignani Alessandro, Tian Huaiyu, Dye Christopher, et al. Modelling COVID-19 *Nature Reviews Physics.* 2020;2:279–281.

25. Bertozzi Andrea L., Franco Elisa, Mohler George, Short Martin B., Sledge Daniel. The challenges of modeling and forecasting the spread of COVID-19 *Proceedings of the National Academy of Sciences.* 2020;117:16732–16738.
26. Giordano Giulia, Blanchini Franco, Bruno Raffaele, et al. Modelling the COVID-19 epidemic and implementation of population-wide interventions in Italy *Nature Medicine.* 2020;26:855-860.
27. Parino Francesco, Zino Lorenzo, Porfiri Maurizio, Rizzo Alessandro. Modelling and predicting the effect of social distancing and travel restrictions on COVID-19 spreading *Journal of The Royal Society Interface.* 2021;18:20200875.
28. Aleta Alberto, Martín-Corral David, Pastore y Piontti Ana, et al. Modelling the impact of testing, contact tracing and household quarantine on second waves of COVID-19 *Nature Human Behaviour.* 2020;4:964–971.
29. Yang Jiannan, Zhang Qingpeng, Cao Zhidong, et al. The impact of non-pharmaceutical interventions on the prevention and control of COVID-19 in New York City *Chaos: An Interdisciplinary Journal of Nonlinear Science.* 2021;31:021101.
30. Gozzi Nicolò, Tizzoni Michele, Chinazzi Matteo, Ferres Leo, Vespignani Alessandro, Perra Nicola. Estimating the effect of social inequalities on the mitigation of COVID-19 across communities in Santiago de Chile *Nature Communications.* 2021;12:1–9.
31. Cardona Stephanie, Felipe Naillid, Fischer Kyle, Sehgal Neil Jay, Schwartz Brad E. Vaccination Disparity: Quantifying Racial Inequity in COVID-19 Vaccine Administration in Maryland *Journal of Urban Health.* 2021:1–5.
32. Albani Vinicius VL, Loria Jennifer, Massad Eduardo, Zubelli Jorge P. The impact of COVID-19 vaccination delay: A data-driven modeling analysis for Chicago and New York City *Vaccine.* 2021;39:6088–6094.
33. Jentsch Peter C, Anand Madhur, Bauch Chris T. Prioritising COVID-19 vaccination in changing social and epidemiological landscapes: a mathematical modelling study *The Lancet Infectious Diseases.* 2021.
34. Truszkowska Agnieszka, Behring Brandon, Hasanyan Jalil, et al. High-Resolution Agent-Based Modeling of COVID-19 Spreading in a Small Town *Advanced Theory and Simulations.* 2021;4:2170005.
35. Truszkowska Agnieszka, Zino Lorenzo, Butail Sachit, et al. Predicting the effects of waning vaccine immunity against COVID-19 through high-resolution agent-based modeling *arXiv preprint arXiv:2109.08660.* 2021.
36. Zhou Ying, Xu Renzhe, Hu Dongsheng, Yue Yang, Li Qingquan, Xia Jizhe. Effects of human mobility restrictions on the spread of COVID-19 in Shenzhen, China: a modelling study using mobile phone data *The Lancet Digital Health.* 2020;2:e417–e424.
37. Sasidharan Manu, Singh Ajit, Torbaghan Mehran Eskandari, Parlikad Ajith Kumar. A vulnerability-based approach to human-mobility reduction for countering COVID-19 transmission in London while considering local air quality *Science of The Total Environment.* 2020;741:140515.
38. Chang Meng-Chun, Kahn Rebecca, Li Yu-An, Lee Cheng-Sheng, Buckee Caroline O, Chang Hsiao-Han. Variation in human mobility and its impact on the risk of future COVID-19 outbreaks in Taiwan *BMC Public Health.* 2021;21:1–10.
39. Wang Ding, He Brian Yueshuai, Gao Jingqin, Chow Joseph YJ, Ozbay Kaan, Iyer Shri. Impact of COVID-19 behavioral inertia on reopening strategies for New York City Transit *International Journal of Transportation Science and Technology.* 2021;10:197–211.
40. Miralles-Pechuan Luis, Ponce Hiram, Martinez-Villasenor Lourdes. Optimization of the Containment Levels for the Reopening of Mexico City due to COVID-19 *IEEE Latin America Transactions.* 2021;19:1065–1073.
41. Lee Serin, Zabinsky Zelda B, Wasserheit Judith N, Kofsky Stephen M, Liu Shan. COVID-19 Pandemic Response Simulation in a Large City: Impact of Nonpharmaceutical Interventions on Reopening Society *Medical Decision Making.* 2021;41:419–429.
42. Truszkowska Agnieszka, Thakore Malav, Zino Lorenzo, et al. Designing the Safe Reopening of US Towns Through High-Resolution Agent-Based Modeling *Advanced Theory and Simulations.* 2021;4:2100157.
43. Bhowmik Tanmoy, Tirtha Sudipta Dey, Iraganaboina Naveen Chandra, Eluru Naveen. A comprehensive analysis of COVID-19 transmission and mortality rates at the county level in the United States considering socio-demographics, health indicators, mobility trends and health care infrastructure attributes *PLOS ONE.* 2021;16:e0249133.
44. Aguilar Javier, Bassolas Aleix, Ghoshal Gourab, et al. Impact of urban structure on COVID-19 spread *arXiv preprint arXiv:2007.15367.* 2020.
45. Brizuela Noel G, García-Chan Néstor, Gutiérrez Pulido Humberto, Chowell Gerardo. Understanding the role of urban design in disease spreading *Proceedings of the Royal Society A.* 2021;477:20200524.
46. Hazarie Surendra, Soriano-Paños David, Arenas Alex, Gómez-Gardeñes Jesús, Ghoshal Gourab. Interplay between population density and mobility in determining the spread of epidemics in cities *Communications Physics.* 2021;4:1–10.
47. Li Xin, Zhou Lin, Jia Tao, Peng Ran, Fu Xiongwu, Zou Yuliang. Associating COVID-19 severity with urban factors: a case study of Wuhan *International Journal of Environmental Research and Public Health.* 2020;17:6712.
48. United States Census Bureau . Explore Census Data `https://data.census.gov/cedsci`.
49. OpenStreetMap Community . OpenStreetMap `https://www.openstreetmap.org` 2021.
50. Google . Google Maps `https://www.google.com/maps` 2021.
51. Institute for Education Science . National Center for Education Statistics `https://nces.ed.gov`.
52. Child Care Centers . Child Care Centers `https://childcarecenter.us/`.
53. School & College Listings . Find Local Schools & Colleges `https://www.schoolandcollegelistings.com/`.
54. Department of Children and Family Services . Facility Search `https://hs.ocfs.ny.gov/DCFS/`.
55. New York State Department of Health . NYS Health Profiles — Montefiore New Rochelle Hospital `https://profiles.health.ny.gov/hospital/view/103001`.
56. American Hospital Directory . Montefiore New Rochelle Hospital `https://www.ahd.com/free_profile/330184/Montefiore_New_Rochelle_Hospital/New_Rochelle/New_York`.
57. SafeGraph Inc. . SafeGraph 2021.
58. Esri . ArcGIS 2021.
59. Washington State Department of Health and Washington State Department of Labor and Industries . COVID-19 Confirmed Cases by Industry Sector December 17, 2020.
60. Washington State Department of Health and Washington State Department of Labor and Industries . COVID-19 Confirmed Cases by Industry Sector November 24, 2021.

61. Ferguson Neil M, Laydon Daniel, Nedjati-Gilani Gemma, et al. Impact of non-pharmaceutical interventions (NPIs) to reduce COVID-19 mortality and healthcare demand Report of the Imperial College London, UK (`https://doi.org/10.25561/77482`) 2020.
62. Kathy Katella . 5 things to know about the Delta variant 2021.
63. Li Baisheng, Deng Aiping, Li Kuibiao, et al. Viral infection and transmission in a large well-traced outbreak caused by the Delta SARS-CoV-2 variant *medRxiv.* 2021.
64. Quilty Billy J, Clifford Samuel, Hellewell Joel, et al. Quarantine and testing strategies in contact tracing for SARS-CoV-2: a modelling study *Lancet Public Health.* 2021;6:e175-e183.
65. The White House . President Biden's COVID-19 Plan `https://www.whitehouse.gov/covidplan/` 2021.
66. European Commission . Public Health 2021.
67. Koh David. Occupational risks for COVID-19 infection *Occupational Medicine.* 2020;70:3.
68. Garzaro Giacomo, Clari Marco, Ciocan Catalina, et al. COVID-19 infection and diffusion among the healthcare workforce in a large university-hospital in northwest Italy *La Medicina del Lavoro.* 2020;111:184.
69. Krishnakumar Balaji, Rana Sravendra. COVID 19 in INDIA: Strategies to combat from combination threat of life and livelihood *Journal of Microbiology, Immunology and Infection.* 2020;53:389–391.
70. The Lancet . COVID-19: protecting health-care workers *The Lancet.* 2020;395:922.
71. Ghorui Neha, Ghosh Arijit, Mondal Sankar Prasad, et al. Identification of dominant risk factor involved in spread of COVID-19 using hesitant fuzzy MCDM methodology *Results in Physics.* 2021;21:103811.
72. Wee LE, Conceicao Edwin Philip, Sim XYJ, et al. Minimizing intra-hospital transmission of COVID-19: the role of social distancing *Journal of Hospital Infection.* 2020;105:113–115.
73. Her Minyoung. Repurposing and reshaping of hospitals during the COVID-19 outbreak in South Korea *One Health.* 2020;10:100137.
74. Yuan Yan, Qiu Tao, Wang Tianyu, et al. The application of Temporary Ark Hospitals in controlling COVID-19 spread: the experiences of one Temporary Ark Hospital, Wuhan, China *Journal of Medical Virology.* 2020;92:2019–2026.
75. Waris Abdul, Atta UK, Ali M, Asmat A, Baset AJNM. COVID-19 outbreak: current scenario of Pakistan *New Microbes and New Infections.* 2020;35:100681.
76. Hur Jian, Chang Min Cheol. Usefulness of an online preliminary questionnaire under the COVID-19 pandemic *Journal of Medical Systems.* 2020;44:1–2.
77. Jnr Bokolo Anthony. Use of telemedicine and virtual care for remote treatment in response to COVID-19 pandemic *Journal of Medical Systems.* 2020;44:1–9.
78. Hsu Suh-Meei, Cheng Tsung-Kuei, Chang Po-Jen, Chen Teng-Yu, Lu Ming-Huei, Yeh Hui-Tzu. Tracking Hospital Visitors/Chaperones during the COVID-19 Pandemic *Applied Clinical Informatics.* 2021;12:266–273.
79. Centers for Disease Control and Prevention . Interim infection prevention and control recommendations for healthcare personnel during the coronavirus disease 2019 (COVID-19) pandemic `https://www.cdc.gov/coronavirus/2019-ncov/hcp/infection-control-recommendations.html`.
80. Zhang Kevin, Shoukat Affan, Crystal William, Langley Joanne M, Galvani Alison P, Moghadas Seyed M. Routine saliva testing for the identification of silent coronavirus disease 2019 (COVID-19) in healthcare workers *Infection Control & Hospital Epidemiology.* 2021:1–5.
81. Stokel-Walker Chris. Covid-19: The countries that have mandatory vaccination for health workers *British Medical Journal.* 2021;373.
82. Hagan Kobina, Forman Rebecca, Mossialos Elias, Ndebele Paul, Hyder Adnan A, Nasir Khurram. COVID-19 Vaccine Mandate for Healthcare Workers in the United States: A Social Justice Policy *Expert Review of Vaccines.* 2021.
83. Centers for Disease Control and Prevention . Quarantine and isolation `https://www.cdc.gov/coronavirus/2019-ncov/your-health/quarantine-isolation.html?CDC_AA_refVal=https\%3A\%2F\%2Fwww.cdc.gov\%2Fcoronavirus\%2F2019-ncov\%2Fif-you-are-sick\%2Fquarantine.html` 2021.

Supplementary Information for **Urban determinants of COVID-19 spread: A comparative study across three cities in New York State**

## S1: Creation of households

All agents who are not residents of retirement homes or hospital patients are assigned a household. Household structure follows the U.S. Census data on housing statistics [17] on household size, percentage of families, single and two-parent families, and fraction of households with senior citizens. Households can be stand-alone buildings or be a part of multiunit structures. Agent location is the same as the geographic coordinates of the household they are assigned to. The geographic coordinates are used to assign each agent a workplace and several non-essential businesses that they may frequent as described in our previous publication [14]. The frequency with which agents visit non-essential businesses is selected as the average value of available records across the three cities, collected during early spring 2021.

To spatially distribute the households, we use the U.S. Census on single and multiunit residential buildings listed in Table S1. Below, we outline the algorithm for generating households and their coordinates

1. **Collect coordinates of all residential buildings**
   Spatial coordinates of the buildings are collected manually using ArcGIS [3].

2. **Create single unit households**
   The number of single unit households, $N_{1\mathrm{H}}$, in our model is

   $$N_{1\mathrm{H}} = N_{1-\mathrm{A}} + N_{1-\mathrm{D}} + N_{\mathrm{M}} + N_{\mathrm{O}}, \tag{S1}$$

   which corresponds to the total number of the relevant U.S. Census categories outlined in Table S1: 1-unit attached ($N_{1-\mathrm{A}}$), 1-unit detached ($N_{1-\mathrm{D}}$), mobile homes ($N_{\mathrm{M}}$), and other ($N_{\mathrm{O}}$), which represents boats, RVs, etc. In this step, we randomly choose locations collected in Step 1 and turn them into single households.

3. **Create two-unit households**
   The number of buildings with two households, $N_{2\mathrm{H}}$, is computed following the data in Table S1 as:

   $$N_{2\mathrm{H}} = \left\lfloor \frac{n_{\mathrm{u},2}}{2} \right\rfloor, \tag{S2}$$

   where $n_{\mathrm{u},2}$ is the number of households located in two unit buildings and $\lfloor \cdot \rfloor$ indicates rounding off to the lowest integer. The buildings are then randomly assigned to the locations that were not selected as 1-unit in Step 2. Each of such geographic locations will thus have two households assigned to it.

4. **Create households characterized by ranges of units**
   Part of the multi-unit structures in the U.S. Census data are characterized by a range of units, for example, 5–9. To create those households, we

   (a) Select the average number of units in the building, $n_{\mathrm{i}}$ that is within the reported range as listed in Table S1.

   (b) Calculate the number of buildings with $n_{\mathrm{i}}$ units, $N_{\mathrm{iH}}$:

   $$N_{\mathrm{iH}} = \left\lfloor \frac{n_{\mathrm{u,i}}}{n_{\mathrm{i}}} \right\rfloor, \tag{S3}$$

   where $n_{\mathrm{u,i}}$ is the number of units in buildings with $n_{\mathrm{i}}$ households.

   (c) If enough locations are available after assigning single- and two-unit households, randomly assign $N_{\mathrm{iH}}$ buildings to a subset of the same

   (d) If there are not enough available locations, randomly select $N_{\mathrm{iH}}$ buildings with more than one unit and add $n_{\mathrm{i}}$ households to them.

5. **Generate households with more than 20 units**
   For multi-unit buildings that represent complexes with 20 or more households, we follow a procedure similar to that summarized above, specifically,

   (a) Calculate the number of buildings with at least 20 units, $N_{\mathrm{20H}}$:

   $$N_{\mathrm{20H}} = \left\lfloor \frac{n_{\mathrm{u,20}}}{20} \right\rfloor + N_{\mathrm{E}}. \tag{S4}$$

   where $n_{\mathrm{u,20}}$ is the number of units in buildings with 20 or more households and $N_{\mathrm{E}}$ is the number of buildings remaining due to rounding operations in the previous steps.

   (b) If there are enough available locations, randomly assign $N_{\mathrm{20H}}$ buildings to have 20 household each and create the households.

   (c) If there are not enough locations, randomly select $N_{\mathrm{20H}}$ buildings with more than one unit and add 20 households to them. This will create buildings with more than 20 households, which is still consistent with the data reported in U.S. Census.

The approach described here is different from how residential building capacity was collected in our previous work [13]. Specifically, in our previous work, multi-unit buildings were identified manually and the number of units within them were estimated based on the floor count of each structure. While our current approach involves significantly less manual assignment, it also results in a more evenly distributed population. To verify that this coarser approach of household assignment does not skew our analysis, we compare the spread of infection along three different testing efficacies in the city of New Rochelle created using manual assignment of household capacity with that using the approach described here. Figure S1 shows the number of active cases, infections, and deaths over a three-month period for three different testing and detection efficacies. Results indicate close agreement between the two approaches, effectively validating the simplified strategy for household capacity assignment for small urban areas.

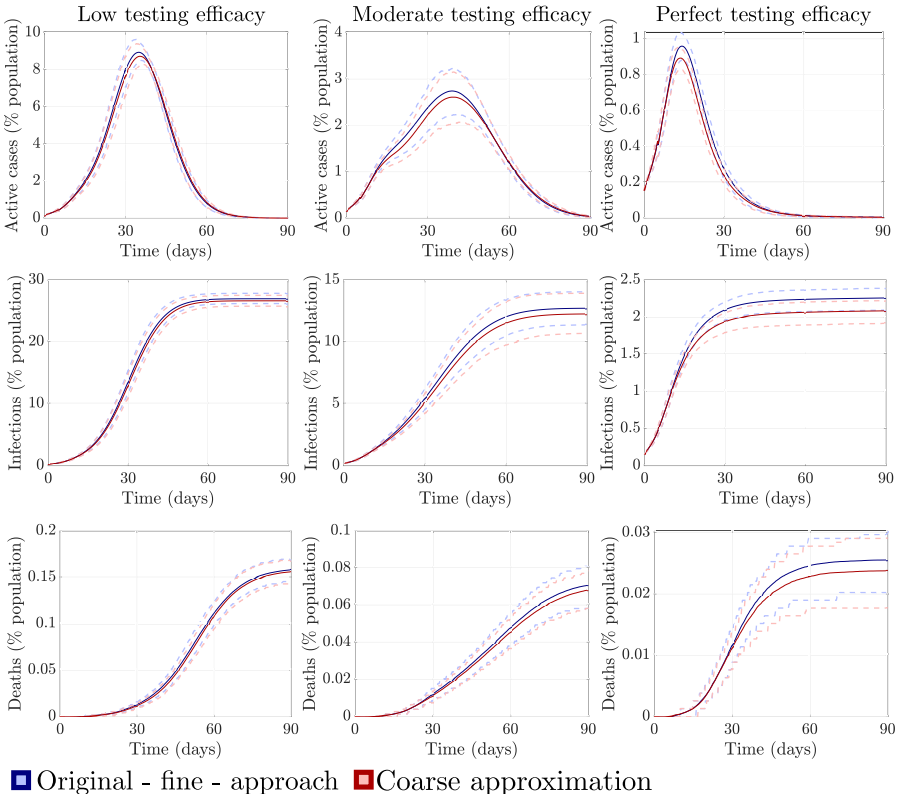


Figure S1: Simulation of the spread of COVID-19 in New Rochelle using manual assignment of household capacity and location, as implemented in our previous study [13], (blue curves) and the random assignment proposed in this work (red curves) over a time-window of three months, for three different testing and detection efficacies. Solid lines represent the average of of 400 independent realizations; dashed lines are the $25^{\text{th}}$ and $75^{\text{th}}$ percentiles.

| **Units in structure** | $n_{\mathrm{i}}$ | **Colonie,** $n_{\mathrm{u,i}}$ | **New Rochelle,** $n_{\mathrm{u,i}}$ | **Utica,** $n_{\mathrm{u,i}}$ |
|---|---|---|---|---|
| 1-unit attached, $N_{1-\mathrm{A}}$ | 1 | 1,150 | 1,364 | 959 |
| 1-unit detached, $N_{1-\mathrm{D}}$ | 1 | 23,273 | 10,316 | 10,774 |
| Mobile home, $N_{\mathrm{M}}$ | 1 | 448 | 0 | 79 |
| Other, $N_{\mathrm{O}}$ | 1 | 0 | 0 | 0 |
| 2 units | 2 | 2,152 | 1,749 | 7,881 |
| 3-4 units | 3 | 1,240 | 3,676 | 3,428 |
| 5-9 units | 7 | 1,269 | 623 | 1,646 |
| 10-19 units | 14 | 2,481 | 1,127 | 699 |
| 20+ units | 20 | 4,551 | 10,791 | 2,703 |

Table S1: U.S. Census data on housing units characteristics used in this work. We do not cite the exact tables as the reported data is subject to regular changes.

| **Occupation category** | **Colonie**, % | **New Rochelle**, % | **Utica**, % |
|---|---|---|---|
| Management, business, science, and art | 47.75 | 47.84 | 28.35 |
| Service | 16.15 | 16.59 | 28.5 |
| Sales and office | 23.67 | 19.31 | 21.98 |
| Natural resources, construction, and maintenance | 5.37 | 6.19 | 6.63 |
| Production, transportation, and material moving | 7.07 | 10.05 | 14.55 |

Table S2: U.S. Census occupational data in the three cities used in our work.

## S2: distribution of agent occupation types

Here, we summarize the procedure for assigning occupation types to the agents using U.S. Census statistics. Occupation types and percentages of people employed in them are listed in Table S2.

Agents are assigned workplaces as follows: we first assign occupations to in-city employees; next, we determine occupations of the agents working out-of-city such as to match the U.S. Census statistics on occupational types shown in Table S2.

## S3: transmission rates for different occupational categories

Agents modeling employees can either work in the city or in its vicinity, with workplaces contributing to an agent's total risk of infection. At any time step, a working susceptible agent can get infected with COVID-19 at time $t$ with the

probability

$$p_i(t) := 1 - e^{-\Delta t \Lambda_i(t)}, \tag{S5}$$

where $\Delta t = 0.25$ day is the duration of a time-step. $\Lambda_i(t)$ represents a combined risk from all the locations that the agent $i$ is associated with,

$$\begin{aligned}\Lambda_i(t) :=& \lambda_{\mathrm{Hh},f_{\mathrm{Hh}}(i)}(t) + \lambda_{\mathrm{W},f_{\mathrm{W}}(i)}(t) + \lambda_{\mathrm{Sc},f_{\mathrm{Sc}}(i)}(t) + \lambda_{\mathrm{Rh},f_{\mathrm{Rh}}(i)}(t) \\ &+ \lambda_{\mathrm{Hsp},f_{\mathrm{Hsp}}(i)}(t) + \lambda_{\mathrm{Tr},f_{\mathrm{Tr}}(i)}(t) + \lambda_{\mathrm{N},f_{\mathrm{N}}(i,t)}(t),\end{aligned} \tag{S6}$$

where $\lambda_{\bullet,\ell}(t)$ represents the risk of infection at location $\ell$ at time $t$. The possible types of locations are: households - Hh, workplaces - W, schools - Sc, retirement homes - Rh, hospitals - Hsp, public transit and carpooling - Tr, and non-essential businesses - N. Function $f_\bullet(i)$ selects the location type that agent $i$ is assigned to. Below, we explain the workplace contribution, $\lambda_{\mathrm{W},f_{\mathrm{W}}(i)}(t)$, and the reader is referred to our previous publications for further details [13–15].

The infection risk contribution for retirement home, hospital, and school employees is associated with corresponding dedicated terms, $\lambda_{\mathrm{Rh},f_{\mathrm{Rh}}(i)}(t)$, $\lambda_{\mathrm{Hsp},f_{\mathrm{Hsp}}(i)}(t)$, and $\lambda_{\mathrm{Sc},f_{\mathrm{Sc}}(i)}(t)$ respectively. In those cases, the generic workplace contribution is set to zero, that is, $\lambda_{\mathrm{W},f_{\mathrm{W}}(i)}(t) = 0$. If an agent works in a generic workplace, $\lambda_{\mathrm{W},f_{\mathrm{W}}(i)}(t) \neq 0$ while other contributions will depend if they are a student and are getting tested or treated for COVID-19. The form of the contribution $\lambda_{\mathrm{W},f_{\mathrm{W}}(i)}(t)$ itself depends on whether the agent works in the city or in the region around it.

The workplaces inside the cities have an occupational type assigned to them based on the SafeGraph data used to locate them [12]. The contribution $\lambda_{\mathrm{W},f_{\mathrm{W}}(i)}(t)$ of such a workplace becomes a function of all other agents working at that location,

$$\lambda_{\mathrm{W},\ell}(t) = \frac{1}{n_\ell} \sum_{j:f_{\mathrm{W}}(i)=\ell} \left( E_{j,\mathrm{W}}(t)\rho_j\beta^k_{\mathrm{W}} + Sy_{j,\mathrm{W}}(t)c_j\rho_j\psi_{\mathrm{W}}\beta^k_{\mathrm{W}} \right), \tag{S7}$$

where $E_j$ and $Sy_j$ are indicator functions that identify when an agent is exposed or symptomatic, respectively; $\rho_j \geq 0$ accounts for the variability in infectiousness among the agents; $c_j > 1$ reflects the increased infectiousness of a symptomatic agent compared to an exposed one; $\psi_{\mathrm{W}}$ denotes the fraction of agents who will still be present at their workplace, regardless of having COVID-19 symptoms; and $\beta^k_{\mathrm{W}}$ is the transmission rate of the workplace of occupational type $k$, as outlined in Table S2. This transmission rate may, in principle, differ among workplaces of various types, reflecting the unequal infection risk in them. For in-city workplaces, $\beta^k_{\mathrm{W}}$ is tied to a specific location and applies to any agent working in that particular workplace. That is, for agent $i$ working in an in-city workplace, the $\beta^k_{\mathrm{W}}$ in Equation S7 has the value that corresponds to that workplace occupational type.

Infection risk from working out-of-city is approximated as

$$\lambda_{\mathrm{WO}} = \beta^k_{\mathrm{W}}\chi_I, \tag{S8}$$

where $\beta_{\mathrm{W}}^{k}$ is the transmission rate for occupation type $k$ and $\chi_I$ is the regional COVID-19 prevalence, estimated from officially reported data for the entire region in vicinity of the city, where the agents work.

In our model, all agent occupations are characterized by their own transmission rates, $\beta_{\mathrm{W}}^{k}$, reflecting different working conditions and their associated infection risks. To compute them, we use empirical data published by the Washington State Department of Health [20, 21] on positivity rates recorded within different occupational categories. The report groups occupations using the North American Industry Classification System (NAICS) [18], as opposed to our categorization which relies on U.S. Census Bureau Occupational Codes [16]. To utilize the results from the report, we group the NAICS occupations into the U.S. Census defined categories utilized in our model, as outlined in Table S3. We then set the positivity rate associated with each category to an average value across all grouped occupations as detailed in Table S4.

To calculate the infection rates for each occupational type $k$, we use scaling relative to the healthcare employees,

$$\beta_{\mathrm{W}}^{i} = \frac{\overline{\chi}^{i}}{\chi^{\mathrm{HSP}}} \beta_{\mathrm{HSP}}. \tag{S9}$$

Here, $\overline{\chi}^{i}$ is the average percentage of COVID-19 cases reported for industry categories classified under occupation $i$, $\chi^{\mathrm{HSP}}$ is the percentage of infected healthcare workers, and $\beta_{\mathrm{HSP}}$ is our previously established healthcare employees transmission rate.

For consistency, we apply this procedure to recompute the original infection rates for school and retirement home employees. The NAICS classification and rates for these categories are also shown in Tables S3 and S4.

# S4: Model parameters

The model parameters used in our work can be found in our previous publication [14]. Here, we list only the parameters that unique to this work except the workplace-related transmission rates that are already detailed in Section . Specifically, we report transmission rates adjusted to reflect the spread of the more infectious Delta variant [7].

[1] Scaled down to city size, time-step, and doubled following calibrated percentage of asymptomatic adults in Ref. [13], used as a proxy for underdetection.

[2] Scaled down to city size, time-step, and doubled following calibrated percentage of asymptomatic adults in Ref. [13], used as a proxy for underdetection; computed based on the total number of cases recovering from COVID-19 during an average recovery period used in Ref. [13]

[3] Scaled down to city size and time-step.

[4] Average over all the areas where the people from a city work and scaled down to a time-step.

## Supplementary References


[1] COVID-19 Forecast Hub. COVID-19 Connecticut weekly forecast summary. https://covid19forecasthub.org/reports/single_page.html?state=CT&week=2021-03-30#County_level.

[2] COVID-19 Forecast Hub. COVID-19 New York weekly forecast summary. https://covid19forecasthub.org/reports/single_page.html?state=NY&week=2021-03-30#County_level.

[3] Esri. ArcGIS, 2021.

[4] Neil M Ferguson, Derek AT Cummings, Christophe Fraser, James C Cajka, Philip C Cooley, and Donald S Burke. Strategies for mitigating an influenza pandemic. *Nature*, 442:448–452, 2006.

[5] Google. COVID-19 Community Mobility Report for New York, March 31, 2021. https://www.gstatic.com/covid19/mobility/2021-03-31_US_New_York_Mobility_Report_en.pdf.

[6] Google News. COVID-19 statistics for Westchest County, NY. https://news.google.com/covid19/map?hl=en-US&mid=%2Fm%2F0cymp&gl=US&ceid=US%3Aen, 2021.

[7] Kathy Katella. 5 things to know about the Delta variant, 2021.

[8] Wee Chian Koh, Lin Naing, Liling Chaw, Muhammad Ali Rosledzana, Mohammad Fathi Alikhan, Sirajul Adli Jamaludin, Faezah Amin, Asiah Omar, Alia Shazli, Matthew Griffith, et al. What do we know about SARS-CoV-2 transmission? a systematic review and meta-analysis of the secondary attack rate and associated risk factors. *PLOS One*, 15(10):e0240205, 2020.

[9] Stephen A. Lauer, Kyra H. Grantz, Qifang Bi, Forrest K. Jones, Qulu Zheng, Hannah R. Meredith, Andrew S. Azman, Nicholas G. Reich, and Justin Lessler. The incubation period of coronavirus disease 2019 (COVID-19) from publicly reported confirmed cases: estimation and application. *Ann. Intern. Med.*, 172:577–582, 2020.

[10] Baisheng Li, Aiping Deng, Kuibiao Li, Yao Hu, Zhencui Li, Qianling Xiong, Zhe Liu, Qianfang Guo, Lirong Zou, Huan Zhang, et al. Viral infection and transmission in a large well-traced outbreak caused by the Delta SARS-CoV-2 variant. *medRxiv*, 2021.

[11] New York State - official website. COVID-19 Vaccine Tracker, 2021.

[12] SafeGraph Inc. SafeGraph, 2021.

[13] Agnieszka Truszkowska, Brandon Behring, Jalil Hasanyan, Lorenzo Zino, Sachit Butail, Emanuele Caroppo, Zhong-Ping Jiang, Alessandro Rizzo, and Maurizio Porfiri. High-resolution agent-based modeling of COVID-19 spreading in a small town. *Adv Theory Simul.*, 4(3):2170005, 2021.

[14] Agnieszka Truszkowska, Malav Thakore, Lorenzo Zino, Sachit Butail, Emanuele Caroppo, Zhong-Ping Jiang, Alessandro Rizzo, and Maurizio Porfiri. Designing the safe reopening of us towns through high-resolution agent-based modeling. *Adv Theory Simul.*, 4(9):2100157, 2021.

[15] Agnieszka Truszkowska, Lorenzo Zino, Sachit Butail, Emanuele Caroppo, Zhong-Ping Jiang, Alessandro Rizzo, and Maurizio Porfiri. Predicting the effects of waning vaccine immunity against covid-19 through high-resolution agent-based modeling. *arXiv preprint arXiv:2109.08660*, 2021.

[16] United States Census Bureau. American Community Survey and Puerto Rico Community Survey, 2020 Code List.

[17] United States Census Bureau. Explore Census Data. `https://data.census.gov/cedsci`.

[18] United States Census Bureau. North American Industry Classification System - NAICS.

[19] United States Census Bureau. QuickFacts, Westchester County, New York; United States. `https://www.census.gov/quickfacts/fact/table/westchestercountynewyork,US/PST045219`.

[20] Washington State Department of Health and Washington State Department of Labor and Industries . COVID-19 Confirmed Cases by Industry Sector, December 17, 2020.

[21] Washington State Department of Health and Washington State Department of Labor and Industries . COVID-19 Confirmed Cases by Industry Sector, November 24, 2021.

| **Occupational category from U.S. Census [16] and this work** | **NAICS categories [18]** |
|---|---|
| Management, business, science, and art | • Finance and insurance<br>• Public administration<br>• Professional, scientific, and technical services<br>• Information |
| Service | • Other services<br>• Arts, entertainment, and recreation<br>• Accommodation and food services<br>• Administrative, support, waste management, and remediation services |
| Sales and office | • Retail trade<br>• Wholesale trade<br>• Information<br>• Professional, scientific, and technical services |
| Natural resources, construction, and maintenance | • Agriculture, forestry, fishing, and hunting<br>• Construction<br>• Mining |
| Production, transportation, and material moving | • Manufacturing<br>• Transportation and warehousing |
| School employees | Educational services |
| Retirement home employees | • Healthcare and social assistance<br>• Accommodation and food services<br>• Other services |

Table S3: Grouping of NAICS categories into occupation classification used in this work.

| **Occupational category** | **Transmission rate**, $\beta_{\mathrm{W}}^{k}$ |
|---|---|
| Healthcare employees | 2.05 |
| Management, business, science, and art | 0.2347 |
| Service | 0.3413 |
| Sales and office | 0.3627 |
| Natural resources, construction, and maintenance | 0.7253 |
| Production, transportation, and material moving | 0.6827 |
| School employees | 0.3413 |
| Retirement home employees | 0.9958 |

Table S4: Grouping of NAICS categories into occupation classification used in this work.

| **Parameter** | **Value** | **References** |
|---|---|---|
| Household transmission rate - untreated | 1.1 $\text{day}^{-1}$ | [4] scaled by 1.41 |
| Household transmission rate - home-isolated | 0.768 $\text{day}^{-1}$ | Assumption |
| Retirement home resident transmission rate - untreated | 1.1 $\text{day}^{-1}$ | Assumption |
| Retirement home resident transmission rate - home-isolated | 0.768 $\text{day}^{-1}$ | Assumption |
| School student transmission rate | 2.13 $\text{day}^{-1}$ | [4] scaled by 1.41 |
| Transmission rate of hospital patients with a condition different than COVID-19 | 2.21 $\text{day}^{-1}$ | Estimated based on data from a clinical consultant |
| Transmission rate of hospitalized agents | 1.63 $\text{day}^{-1}$ | Estimated based on data from a clinical consultant |
| Transmission rate of ICU hospitalized agents | 2.14 $\text{day}^{-1}$ | Estimated based on data from a clinical consultant |
| Transmission rate of infected hospital visitors being tested for COVID-19 | 2.8 $\text{day}^{-1}$ | Estimated based on data from a clinical consultant |
| Transmission rate of agents in a carpool | 1.1 $\text{day}^{-1}$ | Assumed to be equal to $\beta_{\text{Hh,Ut}}$ |
| Transmission rate of agents visiting other agents households | 1.1 $\text{day}^{-1}$ | Assumed to be equal to $\beta_{\text{Hh,Ut}}$ |
| Transmission rate of agents visiting non-essential businesses | 0.3648 $\text{day}^{-1}$ | [8] |

Table S5: COVID-19 transmission parameters. Assumed values were based on discussions with Clinical consultant. Transmission rates where additionally scaled by a factor of 1.6 to reflect the increased infectiousness of the then dominant Delta variant [7].

| Parameter | Value | References |
|---|---|---|
| Latency period | log-normal distribution with 1.225 mean and 0.418 standard deviation, days | [9, 10] |
| Fraction of the population initially infected in the city | $1.32 \times 10^{-4}$ | [2][1] |
| Fraction of agents that are initially active COVID-19 cases | $1.39 \times 10^{-3}$ | [6][2] |
| Fraction of agents that are initially vaccinated | 0.217 | [11][3] |
| Current vaccination rate in the city, %(population)/day | 0.58 | [11] |
| Fraction of the population that is estimated to be infected in the area at a time-step, $\chi_I$ | $1.32 \times 10^{-4}$ | [1, 2, 19][4] |
| Current capacity of public transit compared to its maximum capacity, $\zeta$ | 0.697 | [5] for public transit |
| Fraction of the nominal transmission rate at workplaces, public transit, carpools, and leisure locations associated with current reopening stage (Phase 4) | 0.63 | [5] for workplaces |
| Initial fraction of agents going to leisure locations at each time-step, $\underline{\beta}_{\mathrm{N}}$ | 0.2 | Assumption |
| Final fraction of agents going to leisure locations at each time-step, $\underline{\beta}_{\mathrm{N}}$ | 0.2 | Assumption |

Table S6: Other parameters. The fractions and the vaccination rate are averages of reported data across the three cities. The city populations are 82,797, 79,205, and 59,750 for Colonie, New Rochelle, and Utica, respectively [17].